










Cite this: *Green Chem.*, 2021, **23**, 3127

## Use of ensiled biomass sorghum increases ionic liquid pretreatment efficiency and reduces biofuel production cost and carbon footprint†

Harsha D. Magurudeniya, <sup>a,b</sup> Nawa Raj Baral, <sup>a,c</sup> Alberto Rodriguez, <sup>a,b</sup> Corinne D. Scown, <sup>a,c</sup> Jeff Dahlberg,<sup>a,d</sup> Daniel Putnam,<sup>a,e</sup> Anthe George, <sup>a,b</sup> Blake A. Simmons <sup>a,c</sup> and John M. Gladden <sup>\*a,b</sup>

Pretreatment is an essential step to enable the efficient conversion of lignocellulosic biomass to biofuels and bioproducts. The most effective pretreatment methods currently in use are based on severe thermochemical approaches, which are costly and energy-intensive. Here we explored whether the common practice of ensiling grassy biomass, such as sorghum, could be used as a pre-processing step to increase the conversion efficiency under milder pretreatment conditions. We determined the impact of replacing dry sorghum biomass with ensiled sorghum biomass on the deconstruction efficiency, process economics, and carbon footprint of a lignocellulosic biorefinery that employs a separation-free ionic liquid pretreatment coupled to enzymatic saccharification and microbial conversion. Our results indicate that the use of ensiled biomass allowed for a 50% reduction in both the amount of ionic liquid (from 5 to 2.5% (w/w) as measured by initial pretreatment loading) and the time required for enzymatic saccharification (from 72 h to 24 h) without sacrificing efficiency. We show that the resulting hydrolysate can be used to cultivate an engineered strain of *Rhodospiridium toruloides* to convert >90% of the monomeric sugars into bisabolene, a promising intermediate to biofuels and bioproducts. Overall, we estimate that the replacement of field-dried biomass sorghum with ensiled sorghum in combination with an ionic liquid-based deconstruction process could reduce the minimum selling price and carbon footprint of biofuel production in a biorefinery by at least 13% and 8.2%, respectively.

Received 25th September 2020,  
Accepted 10th February 2021

DOI: 10.1039/d0gc03260c

rsc.li/greenchem

## 1. Introduction

The development of efficient technologies for biomass deconstruction and conversion into high-value products has become increasingly important to facilitate the transition into a sustainable economy. Pretreatment is an essential step to achieve a high-yield conversion of the carbon stored in lignocellulosic biomass into biofuels and other products.<sup>1–3</sup> Common pretreatment methods require high temperatures and pressures to effectively disrupt the structural integrity of biomass, which makes them costly and energy demanding.<sup>4–7</sup> In addition,

high-severity pretreatment conditions could require extensive water washing prior to saccharification to reduce the concentration of enzymatic and microbial inhibitors that may be formed during the process.<sup>8</sup> Hence, the development of cheaper and more efficient pretreatment approaches remain a key challenge for lignocellulosic conversion technologies.

In addition to efficient pretreatment methods, stable storage of biomass for year-round operation is essential to minimize dry matter losses upstream of the biorefinery. Year-round storage of wet biomass (moisture content of 60–75%) is a common practice to maintain an uninterrupted supply of animal feedstock for livestock operations around the world. Despite the focus on dry storage for bioenergy applications, wet biomass has several benefits relative to dry biomass, including lower risk of fire during storage, a wider harvest window, better flexibility to optimize quality, lower soil or dirt contamination, avoidance of damage due to rain, and less material loss during the field operations.<sup>9</sup> Ensiling is a preferred method of biomass preservation for corn, sorghum or other difficult-to-dry biomass crops, especially in rainy regions.<sup>10</sup> This is a well-known farming method, with over

<sup>a</sup>Joint BioEnergy Institute, Lawrence Berkeley National Laboratory, 5885 Hollis St, Emeryville, CA 94608, USA. E-mail: jmgladden@lbl.gov

<sup>b</sup>Sandia National Laboratories, 7011 East Ave, Livermore, CA 94551, USA

<sup>c</sup>Biological Systems and Engineering Division, Lawrence Berkeley National Laboratory, Berkeley, CA 94720, USA

<sup>d</sup>UC-ANR Kearney Agricultural Research and Extension Center, Parlier, CA, USA

<sup>e</sup>Department of Plant Sciences MS #1, University of California, 1 Shields Avenue, Davis, CA, USA

† Electronic supplementary information (ESI) available: Additional data inputs and experimental results. See DOI: 10.1039/d0gc03260c



2.6 million ha of corn and 134 000 ha of sorghum ensiled in 2019.<sup>11</sup>

However, improper storage of wet biomass may result in dry matter losses. Ensiling creates an anaerobic environment that is proven to preserve the quality of wet biomass for longer periods of time. Inoculated or naturally occurring bacteria produce organic acids in this environment, mainly lactic and acetic acids, which are not only beneficial for biomass preservation but also enhance its digestibility for cattle, sheep and other ruminants.<sup>9,12,13</sup> Considering that these organic acids are known to partially decompose cellulose and hemicellulose under certain conditions, the use of ensiled wet biomass could be advantageous for cellulosic biorefineries, specifically in processes that require large amounts of water, which is required for downstream saccharification and conversion. One study evaluated whether ensiled biomass could be used without additional pretreatment and directly added glycoside hydrolyase enzymes to several ensiled feedstocks including barley, triticale, wheat straw, cotton stalks, and triticale hay, and reported sugar yields of 40–45%.<sup>14</sup> They suggest that ensiled biomass feedstocks will require additional pretreatment to break up the complex lignocellulosic structure prior to enzymatic hydrolysis, but the moderate sugar yields indicate that lower severity pretreatments may potentially be effective. Other studies have obtained higher glucose and xylose yields from ensiled biomass relative to dry biomass when enzymatic hydrolysis was coupled with a hot water pretreatment. Oleskiewicz-Popiel *et al.* used hot water pretreatment at 190 °C for the ensiled grass mixtures of clover, maize, and rye and achieved glucose yields in the range of 55–60%, which are 15–20% higher than the direct saccharification.<sup>15</sup> Ensiling of wheat straw prior to performing a hot water pretreatment also resulted in higher sugar yields relative to the unensiled biomass, however, these yields are still considered to be too low for cost-efficient biofuel production.<sup>16,17</sup>

In addition, high temperatures and long reaction times required for effective hydrothermal pretreatment could cause sugar degradation into by-products, impacting the saccharification yields and producing microbial fermentation inhibitors such as furfural and hydroxymethylfurfural.<sup>8</sup> Although the organic acids content in the ensiled biomass could minimize degradation of hydrolyzed sugars to inhibitors when compared to inorganic acids (such as sulfuric acid), they may be toxic to organisms, such as *Saccharomyces cerevisiae*, and result in low ethanol yields.<sup>18,19</sup> The use of ionic liquids (ILs) as pretreatment agents has received increasing interest because of their ability to fractionate and deconstruct lignocellulosic biomass.<sup>20</sup> In particular, our group has developed a one-pot process that combines IL pretreatment using aqueous solutions of the IL, cholinium lysinate [Ch][Lys], with enzymatic saccharification, without the need for washing or separating the biomass slurry before bioconversion. This process has proven to be effective in solubilizing lignin and enabling the action of cellulase and hemicellulase enzymatic cocktails to release monomeric sugars at high titers and yields.<sup>21,22</sup> When coupled to a fermentation step, the majority of sugars and

acids released by this treatment can be converted into biofuels and bioproducts by IL-tolerant organisms such as the oleaginous yeast *Rhodospiridium toruloides*.<sup>21,23</sup>

Recovery of both the IL and the unutilized lignin-rich fraction of biomass after conversion to biofuel is needed to enhance process economics and reduce the carbon footprint of the process. The unutilized lignin-rich biomass can be used to generate onsite process heat and electricity or could be upgraded into biofuels or commodity chemical compounds.<sup>24</sup> Recovery and recycling of ionic liquids is still a significant challenge in many cases. However, previous studies have demonstrated recovery and recycling of about 99% of the IL using a pervaporation-based process.<sup>25</sup>

Here we tested the hypothesis that the combination of both biomass pre-processing through ensiling and one-pot pretreatment can increase biomass deconstruction efficiency without reducing hydrolysate compatibility with downstream biological conversion. This study focused on the effects of IL loading, pH values for saccharification, enzyme loading, and reaction time on pretreatment and conversion efficiency. The biocompatibility of the ensiled biomass hydrolysates was confirmed by cultivating them with an engineered strain of *R. toruloides* that produces the D2 diesel alternative and jet fuel precursor bisabolene. Lastly, we performed a techno-economic analysis and life-cycle assessment to evaluate the impact of this new process on the production cost and carbon footprint of biofuel.

## 2. Results and discussion

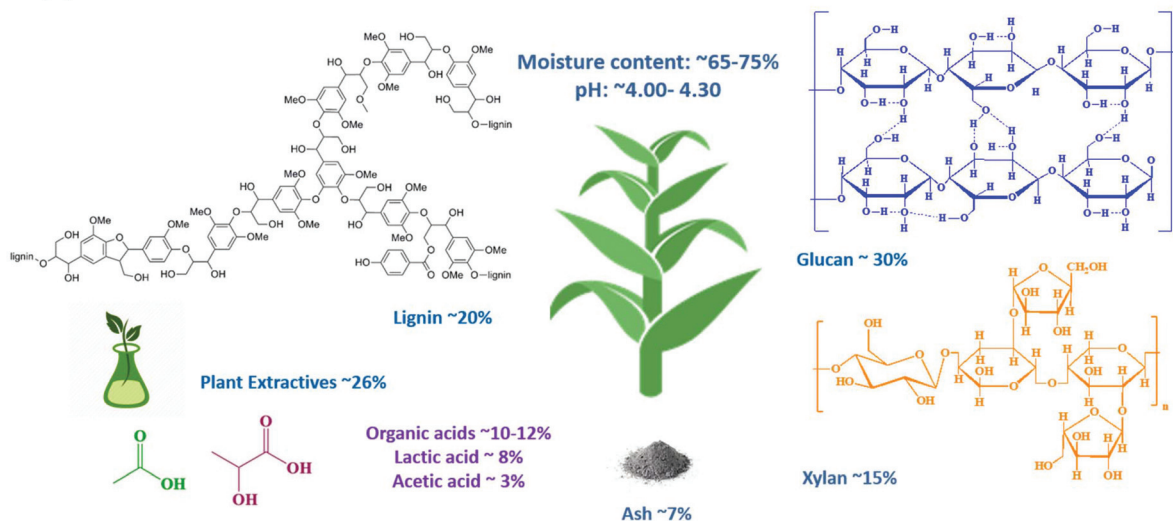
### 2.1. Compositional analysis of dry and ensiled biomass sorghum

Biomass compositional analysis is required to understand the quality and nature of feedstocks for any biomass conversion processes. The compositional analysis of dry sorghum (DS) and ensiled sorghum (ES) revealed several expected similarities and differences between the feedstocks.<sup>26,27</sup> They had similar glucan, xylan and lignin contents, with DS slightly higher in each. The ES contained high moisture in the range of 65 to 75% (w/w), while the moisture content of the field DS is approximately 20% (w/w). The anaerobic fermentation during the ensiling process (wet storage) generates weak organic acids, which brings down the ensiled biomass pH to a value close to 4, while the pH of the DS stays around 7. Fig. 1 summarizes the detailed composition analysis of both ES and DS feedstocks.

One of the key differences between both feedstocks is the extractive content (Fig. 1B). The DS contained around 18% of extractives, which are primarily monosaccharides such as glucose, fructose and smaller amounts of xylose, galactose, and arabinose. In contrast, the extractive content in the ES material reached 26%, mainly due to higher amounts of lactic (8–9%) and acetic (3–4%) acids, despite having a relatively lower mono- and polysaccharide content (Fig. 1A). These results are not surprising because the microorganisms that are present during the ensiling process ferment the free sugars



## (A) Structural composition of ensiled sorghum biomass



(B)

| Biomass     | Dry sorghum (DS)<br>% (w/w) | Ensiled sorghum (ES)<br>% (w/w) |
|-------------|-----------------------------|---------------------------------|
| Glucan      | 34                          | 30                              |
| Xylan       | 18                          | 15                              |
| Lignin      | 22                          | 20                              |
| Extractives | 18                          | 26                              |
| Ash         | 4                           | 7                               |

Fig. 1 (A) Structural composition of ensiled biomass sorghum; (B) comparison of the compositions of dry sorghum and ensiled sorghum.

into organic acids. The compositional analysis results also show that there is a small reduction in the amount of structural carbohydrates such as cellulose and hemicellulose in the ES, likely due to their partial fermentation.

## 2.2. One-pot IL pretreatment of dry and ensiled biomass sorghum

The biological processes that result in the production of organic acids in ES are thought to partially degrade the biomass or weaken the cellulose-hemicellulose-lignin interlinkages.<sup>35-38</sup> Since biomass pretreatment acts using similar mechanisms, we hypothesized that ES would be more readily deconstructed and require milder pretreatment conditions to achieve high sugar yields. To test this, we compared the deconstruction of dry and ensiled biomass under several different conditions: no pretreatment, hot water pretreatment, and IL pretreatment. The no pretreatment saccharification of both DS and ES was carried out to establish a baseline deconstruction efficiency of the two feedstocks. As expected, DS in the absence of pretreatment produced very low yields of glucose (20% cellulose converted) and xylose (17% xylan converted) after enzymatic hydrolysis (Fig. 2 and Table 1). Meanwhile, ES had increased glucose yields (from 20 to 33%), in agreement with previous reports, but the xylose yields did not increase relative to DS. The benefit of using ensiled

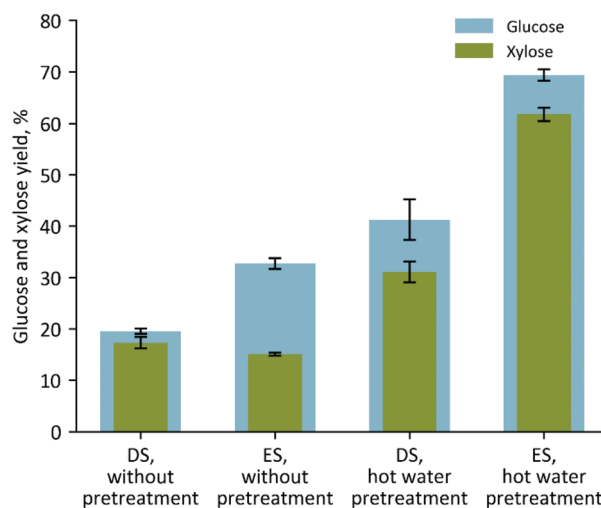


Fig. 2 Glucose and xylose yields obtained from raw (not pretreated) and hot water pretreated dry (DS) or ensiled (ES) sorghum after enzymatic hydrolysis.

material was also observed when conducting a hot water pretreatment where the yields of glucose were 69% for ES and only 41% for DS and for xylose were 62% for ES and only 31% for DS (Fig. 2 and Table 1). In an attempt to further increase



**Table 1** Summary of glucose and xylose yields obtained by performing enzymatic saccharification to dry or ensiled sorghum pretreated with IL, hot water, or not pretreated

| Pretreatment process | Dry sorghum (DS)         |                         | Ensiled sorghum (ES)     |                         |
|----------------------|--------------------------|-------------------------|--------------------------|-------------------------|
|                      | Glucose <sup>a</sup> (%) | Xylose <sup>b</sup> (%) | Glucose <sup>a</sup> (%) | Xylose <sup>b</sup> (%) |
| None                 | 19.54 (±0.54)            | 17.30 (±1.12)           | 32.71 (±1.10)            | 15.08 (±0.29)           |
| Hot Water            | 41.22 (±3.96)            | 31.07 (±2.01)           | 69.38 (±1.11)            | 61.75 (±1.33)           |
| [Ch][Lys] 2.5%       | 67.51 (±2.84)            | 51.78 (±1.35)           | 83.90 (±2.10)            | 62.11 (±0.45)           |
| [Ch][Lys] 5%         | 75.86 (±4.45)            | 60.76 (±2.06)           | 91.54 (±0.98)            | 71.64 (±0.96)           |
| [Ch][Lys] 10%        | 80.52 (±0.16)            | 61.68 (±3.63)           | 87.62 (±0.16)            | 64.26 (±1.92)           |

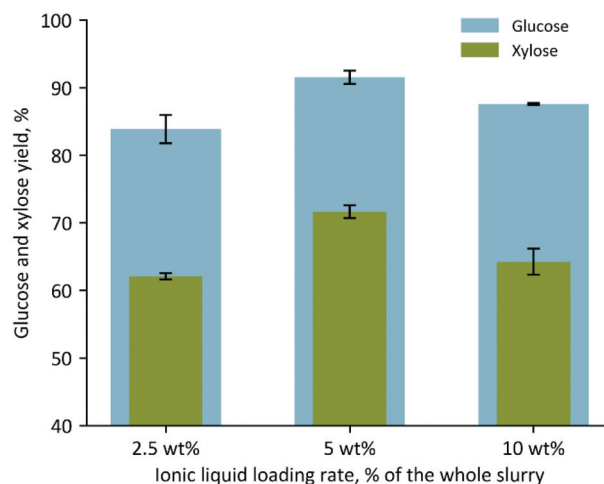
<sup>a</sup> Cellulose conversion based on the composition analysis data presented in Fig. 1(B). <sup>b</sup> Xylan conversion based on the composition analysis data presented in Fig. 1(B).

sugar yields, we investigated the effects of using the ES in a one-pot IL process configuration. The main parameters evaluated in this comparison were the ionic liquid concentration, pH of the saccharification, enzyme loadings, and duration of the hydrolysis reaction.

It has been demonstrated that the cholinium-based ILs cause the delignification of biomass and increase the accessibility of polysaccharides for the enzymatic hydrolysis.<sup>39–41</sup> Therefore, we wanted to determine whether there are differences in lignin extraction during pretreatment in DS vs. ES. Fig. S1† shows the extent of lignin removal after one-pot IL pretreatment of both DS and ES. Regardless of the types of biomass (dry or ensiled), the lignin removal is increased with increased IL loading from 2.5 to 5%, consistent with previously reported observations. The results show that the lignin removal from ES is greater than DS, about 20% and 36% higher after pretreatment with 2.5% and 5% IL, respectively. These results are consistent with the hypothesis that the ensiling process partially degrades the biomass, resulting in fewer polysaccharide-lignin linkages, which would facilitate lignin extraction.

**2.2.1. Effect of ionic liquid loading.** The biomass deconstruction efficiency using three different concentrations of the IL [Ch][Lys] (2.5, 5, and 10% (w/w)) was determined from both DS and ES in a one-pot process configuration. It was found that the presence of IL resulted in higher total monomeric sugar yields in all cases, when compared to the hydrothermal pretreatment (Fig. 3 and Table 1). The highest glucose and xylose yields, 92% and 72%, respectively, were observed with ensiled biomass at an IL concentration of 5%.

These results show that the ES pretreatment resulted in ~20–25% more glucose when compared to the respective DS pretreatment, despite DS having a slightly higher glucan content (Table 1 and Fig. S2†). Interestingly, the xylose yields displayed a lesser improvement and remained below ~70% of the maximum, suggesting that further optimization of the hemicellulase reaction conditions may be necessary to counteract potential enzyme inhibition effects caused by the ionic liquid, organic acids, or other compounds present in ES hydrolysates. The reactions containing 2.5 and 5% IL were also performed at a larger scale using a 1 L Parr reactor and similar values were obtained (Fig. S3†). Reducing the pretreatment

**Fig. 3** Glucose and xylose yields obtained by performing a one-pot process with ES using three different IL concentrations, 2.5, 5, and 10 wt%.

temperature from 140 to 95 °C in the 1 L Parr reaction resulted in slightly lower glucose and xylose yields, 82% and 55%, respectively (Fig. S4†). These experiments suggest that it may be feasible to further scale-up the process with ES and perform the pretreatment at lower temperature and pressure conditions as a cost-saving measure.

**2.2.2. pH adjustment after IL pretreatment.** One important parameter for efficient saccharification is setting a pH value in the range of 4.8 to 5.5 in the slurry at the time of enzyme addition. [Ch][Lys] is a basic IL with a pH of around 12, therefore it is important to minimize the amount used for pretreatment to simplify adjusting the pH to values that are compatible with enzymatic and microbial conversion. In the case of the feedstocks evaluated here, the untreated ES has a pH of 4.3, which is more acidic compared to a value of 7.3 in the DS. As expected, the pH values increased upon addition of the IL and decreased again after pretreatment (Fig. 4). This effect is probably caused by the formation of acidic moieties such as acetic acid resulting from the deacetylation of hemicellulose during pretreatment.<sup>42,43</sup> It can be observed that the use of ES resulted in pH values that are closer to the optimum values



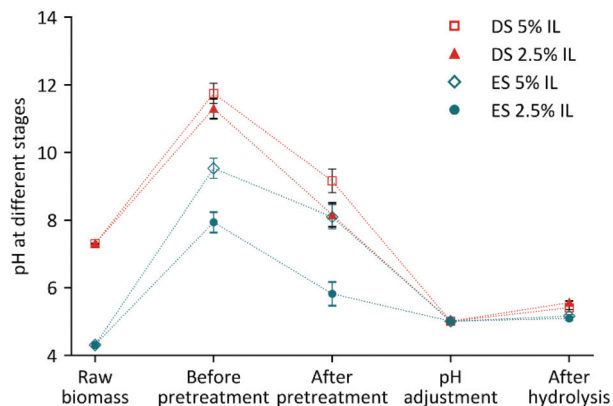


Fig. 4 pH variations at several stages of the biomass deconstruction process.

required for saccharification, compared to DS. Although pre-treating ES with a 5% (w/w) [Ch][Lys] concentration resulted in higher sugar yields, the use of a 2.5% (w/w) concentration resulted in a final pH value of 5.8, making it the only condition that could potentially be saccharified without performing a pH adjustment. This could be another important advantage of ES to reduce capital and operating costs at large scales.

**2.2.3. Enzyme loadings.** Optimization of the fully consolidated IL pretreatment and enzymatic saccharification processes is an important step before commercial deployment. The amount of the enzymes used for saccharification could significantly alter the overall biofuel production cost and greenhouse gas emissions. In order to achieve an economically viable biofuel production technology, the enzyme loading must be reduced while maintaining a high saccharification efficiency. An enzyme loading ratio in the range of 20 or 30 mg of protein per gram of biomass is generally used to achieve high glucose and xylose yields.<sup>31,40,44</sup> Considering that an enzymatic cocktail loading of 10 mg g<sup>-1</sup> of biomass was used in the previous experiments presented in this study, we tested the effect of using an enzyme loading of 20 mg g<sup>-1</sup> on ES pretreated with different IL concentrations (2.5, 5, and 10% (w/w)) for 72 h. For each reaction, the enzyme loadings were normalized to the respective amount of biomass loading used in the pretreatment.<sup>27</sup> It was found that doubling the enzyme concentration from 10 to 20 mg g<sup>-1</sup> of biomass did not significantly affect the sugar conversion for each IL concentration (Fig. 5). Glucose yields showed a slight increase from 83.9 to 86.5%, 91.5 to 95.5% and 87.6 to 89.5% for 2.5, 5, and 10% (w/w) IL concentrations, respectively. A similar behavior was observed for xylose conversion. Interestingly, the xylose yields were not improved upon doubling the enzyme loading and remained at values lower than 72%. These results show that the concentration of IL has a larger effect on sugar yields than the enzyme loading for the tested conditions.

**2.2.4. Enzymatic hydrolysis duration.** As we discussed earlier, using a lower enzyme loading and achieving a high sugar conversion in a one-pot process is a key factor for redu-

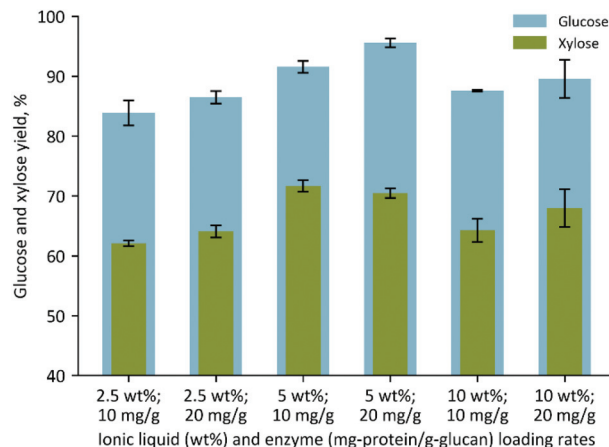


Fig. 5 Effects of different IL concentrations (top values on x-axis, wt%) and enzyme loading ratios (bottom values on x-axis, mg protein per g of biomass) on glucose and xylose yields obtained from ES biomass.

cing the biofuel production cost and greenhouse gas emissions.

At the same time, reducing the enzymatic hydrolysis time may decrease the reactor energy consumption. We monitored the sugar release during the enzymatic hydrolysis of ES and DS biomass pretreated with 2.5% (w/w) [Ch][Lys]. The results show that DS biomass requires 48 to 72 h to reach maximum conversion of polysaccharides to glucose and xylose, while a shorter hydrolysis time, between 24 and 48 h, was sufficient for ES (Fig. 6).

### 2.3. Fermentations on hydrolysates generated using the one-pot process on ES

One crucial parameter for the valorization of lignocellulosic biomass is the compatibility of the biomass hydrolysates with microbial conversion platform organisms. Parameters like the

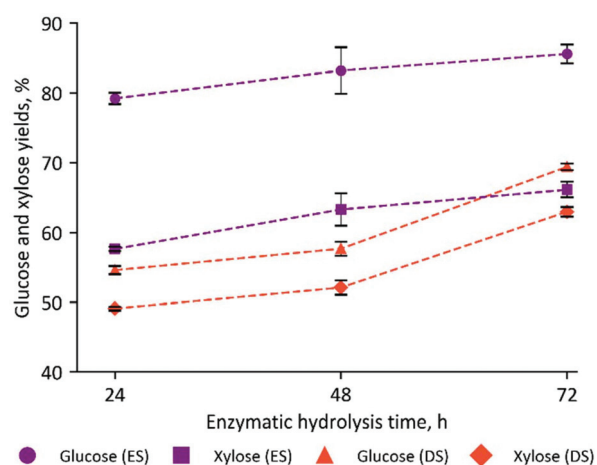


Fig. 6 Glucose and xylose yields measured at different time intervals during the enzymatic hydrolysis of the 2.5% (w/w) [Ch][Lys] IL pretreated ensiled sorghum (ES) and dried sorghum (DS).



type of feedstock, chemicals and conditions used for pretreatment, final pH, and the concentration of inhibitory compounds in the final hydrolysates have a strong influence on the performance of the conversion host.<sup>45</sup> To examine biocompatibility, we evaluated whether the hydrolysates generated under the conditions that promoted the highest sugar release could be used to cultivate *R. toruloides*. This oleaginous red yeast was chosen as a conversion host because it has been previously demonstrated to be tolerant to salts, relatively low pH conditions, and compounds commonly generated during the thermochemical and enzymatic depolymerization of lignocellulosic biomass.<sup>21,46</sup> The fact that this organism does not require any additional vitamins, antibiotics, inducers or amino acid supplements for growth and product formation in hydrolysates also contributes to lower the fermentation costs. In addition, *R. toruloides* is known to be able to utilize glucose, xylose, biomass-derived organic acids, and some aromatic monomers to generate cell biomass rich in lipids and carotenoids, and can be engineered to accumulate non-native bioproducts like terpenoids or peptide-based pigments.<sup>47,48</sup> Because of this naturally advantageous metabolism, an engineered strain with the ability to produce the alternative biofuel bisabolene was generated in a previous study. Bisabolene is a sesquiterpene that upon reduction to bisabolane, can be used as an alternative D2 diesel or jet fuel.<sup>49</sup>

Here we evaluated the performance of this strain as the biofuel producer in a one-pot IL process using ES pretreated with 2.5 and 5% (w/w) IL. Cultivations were set using hydrolysates supplemented only with ammonium sulfate as nitrogen source, and the final cell biomass, substrate consumption and bisabolene production were measured after 5 days of incubation. The toxicity of the media was evaluated by comparing two hydrolysate concentrations, 90% and 50% of the original hydrolysates, after diluting with water. The results of these experiments are shown in Table 2.

We observed that the engineered *R. toruloides* strain displayed robust growth and bisabolene production in the four tested conditions. Table 2 shows that both IL concentrations produced similar amounts of glucose, xylose, lactic acid, and acetic acid, and these compounds were almost completely consumed in all cases, except for lactic acid, which was only par-

tially consumed. Although the final cell biomass did not change significantly when using different IL loadings or hydrolysate concentrations, the bisabolene titers changed proportionally to the amount of substrate present in the diluted hydrolysates before inoculation. These results support the use of pretreated and saccharified ensiled sorghum in a one-pot configuration for biological conversion using a low IL concentration of 2.5% (w/w). The engineered strain did not display any apparent inhibition in growth or production capabilities caused by the more concentrated media, suggesting that it could be possible to implement higher pretreatment solid loadings and avoid hydrolysate dilutions to increase product titers. For comparison, prior studies have reported bisabolene titers of 912 mg L<sup>-1</sup> in *S. cerevisiae*<sup>49</sup> and 800 mg L<sup>-1</sup> (ref. 50) or 1100 mg L<sup>-1</sup> (ref. 51) with engineered strains of *E. coli*.

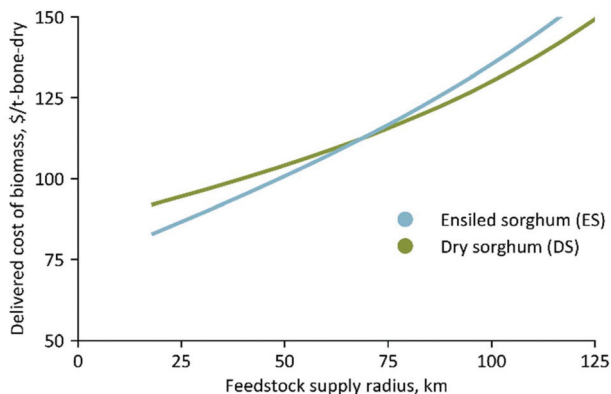
#### 2.4. Minimum selling price and carbon footprint of biofuels

Fig. 7 shows the delivered cost of dry and ensiled biomass sorghum as a function of distance from the field to the biorefinery. This includes the cost associated with biomass production, harvesting, transportation, and storage. Despite dry down from the average moisture content at the time of harvest of 60 to 20% in the field, we find that the ensiled chopped-biomass sorghum supply system is economically feasible for the feedstock supply radius of <65 km (<40 miles) when compared to the dry biomass sorghum supply system in the form of bale (Fig. 7). The costs and losses associated with the dry biomass scenario can increase further if precipitation impacts the dry down process and the bulk density of a bale. The advantage of ensiling is mainly due to the additional costs associated with field drying, baling, and stacking. The location of the biorefinery, local climate, and ease of the downstream conversion process will all impact which feedstock handling scenario is preferable. This study determined the production cost and carbon footprint utilizing the dry and ensiled biomass sorghum feedstocks considering the location of an ethanol biorefinery within an economic cut-off supply radius of 65 km (40 miles). Ethanol was chosen because it is currently deployed biofuel. This distance is equivalent to the feedstock supply radius from field to the biorefinery resulting from the percentage of surrounding land cultivated with sorghum of

**Table 2** Bisabolene titers, final cell biomass and substrate utilization values obtained after cultivation of engineered *R. toruloides* in hydrolysates generated using the ES IL one-pot process

| IL loading (%) (w/w) | Hydrolysate concentration (%) | Bisabolene titer (mg L <sup>-1</sup> ) | Final cell biomass (OD <sub>600</sub> ) | Initial substrate concentration (g L <sup>-1</sup> ) |                   |                    |                   | Bisabolene titer relative to theoretical maximum (%) | Bisabolene yield (% based on dry feedstock) |
|----------------------|-------------------------------|----------------------------------------|-----------------------------------------|------------------------------------------------------|-------------------|--------------------|-------------------|------------------------------------------------------|---------------------------------------------|
|                      |                               |                                        |                                         | Substrate utilization (%)                            |                   |                    |                   |                                                      |                                             |
|                      |                               |                                        |                                         | Glucose                                              | Xylose            | Acetic             | Lactic            |                                                      |                                             |
| 2.5                  | 90                            | 1178 ± 189                             | 13.6 ± 0.2                              | 42.4 ± 0.7                                           | 13.7 ± 0.2        | 4.0 ± 0.0          | 6.7 ± 0.4         | 8.7                                                  | 0.66                                        |
|                      |                               |                                        |                                         | <b>98.4 ± 0.3</b>                                    | <b>92.3 ± 2.0</b> | <b>100.0 ± 0.0</b> | <b>30.7 ± 3.8</b> |                                                      |                                             |
| 5                    | 50                            | 1385 ± 266                             | 13.0 ± 0.2                              | 50.5 ± 0.1                                           | 20.7 ± 0.0        | 4.2 ± 0.0          | 7.5 ± 0.2         | 8.1                                                  | 0.77                                        |
|                      |                               |                                        |                                         | <b>97.3 ± 0.2</b>                                    | <b>92.5 ± 0.4</b> | <b>100.0 ± 0.0</b> | <b>21.9 ± 1.8</b> |                                                      |                                             |
| 2.5                  | 50                            | 583 ± 81                               | 12.3 ± 0.2                              | 22.8 ± 0.1                                           | 7.3 ± 0.1         | 2.1 ± 0.1          | 3.0 ± 0.0         | 8.0                                                  | 0.58                                        |
|                      |                               |                                        |                                         | <b>98.6 ± 0.1</b>                                    | <b>97.2 ± 0.4</b> | <b>100.0 ± 0.0</b> | <b>44.3 ± 0.4</b> |                                                      |                                             |
| 5                    | 90                            | 627 ± 53                               | 11.8 ± 0.4                              | 28.5 ± 0.1                                           | 11.7 ± 0.0        | 2.3 ± 0.0          | 3.9 ± 0.3         | 6.0                                                  | 0.62                                        |
|                      |                               |                                        |                                         | <b>97.6 ± 0.1</b>                                    | <b>95.8 ± 0.3</b> | <b>100.0 ± 0.0</b> | <b>28.0 ± 5.0</b> |                                                      |                                             |



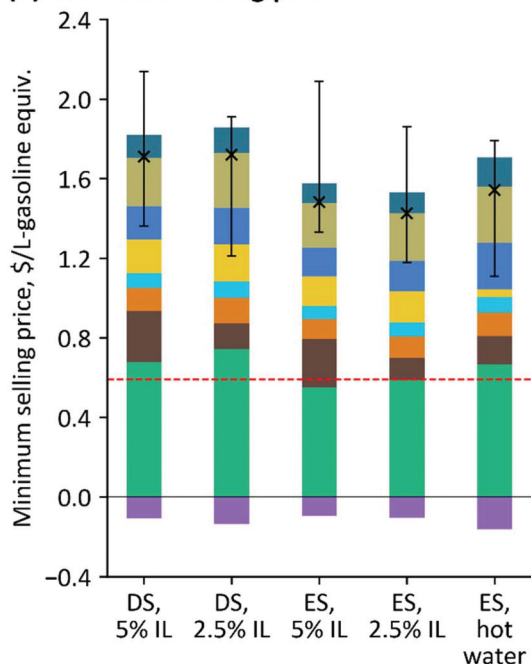


**Fig. 7** Dry sorghum and ensiled sorghum feedstocks supply costs as a function of farm-to-biorefinery distance. The dry feedstock is delivered in the form of bale (20% moisture) and stored next to the biorefinery under the tarp. The ensiled sorghum supply chain includes the direct transportation of chopped biomass (60% moisture) from the field to the biorefinery and ensiled next to the biorefinery in the bunker silo and covered with a tarp. The overall supply cost is presented per bone-dry metric ton (t) of dry or ensiled feedstock.

3.2%, biomass harvest rate of 22.4 metric ton (bone-dry) per ha, and the scale of the biorefinery of 2000 bone-dry metric ton per day.

Utilization of the ES feedstock within the 65 km feedstock collection radius reduces the minimum selling price of ethanol by 13.4% relative to the DS at an IL-loading rate of 5 wt% (based on the whole slurry). This reduction is mainly due to an increased yield of both glucose and xylose (Fig. 3 and Table 1) relative to the DS feedstock. We find that the process is slightly more economical if the IL loading rate is reduced to 2.5 wt%, despite the reduction in sugar yields (Table 1). As illustrated in Fig. 8, the IL cost is a major driver of the minimum selling price, so a dramatic reduction in IL loading can outweigh a minor reduction in sugar yields for the ensiled biomass. However, this is not fully applicable for dry biomass due to a low sugar yield, the non-linear impact of sugar yield on the selling price of biofuel, and nominal cost credit from the biogenic electricity generated from the unutilized biomass. Using a 2.5 wt% IL loading reduces the minimum selling price of ethanol by 17.2% relative to the DS and reduces the selling price by 7.6% relative to the liquid hot

**(a) Minimum selling price**



**(b) Greenhouse gas footprint**

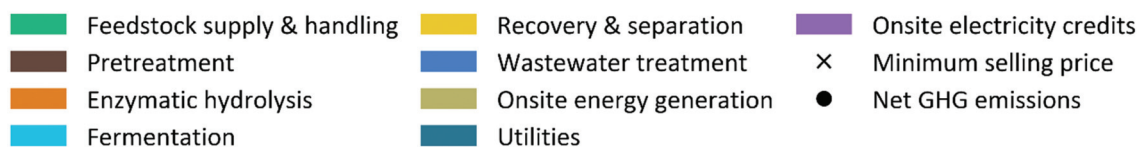
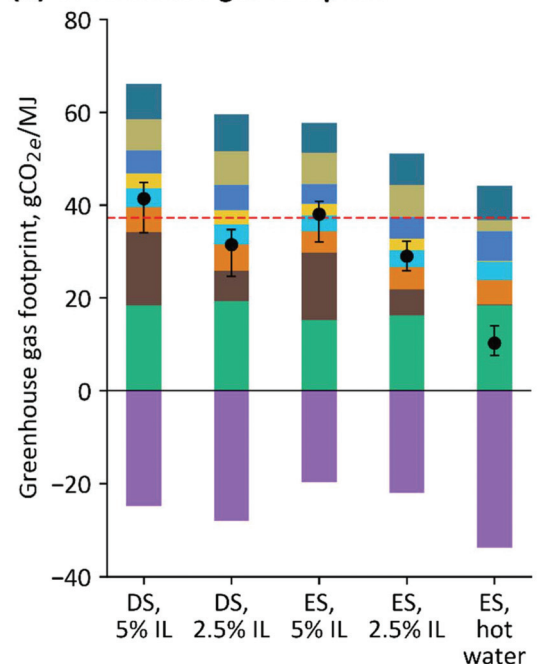


**Fig. 8** Minimum selling price and greenhouse gas footprint of ethanol utilizing dry sorghum (DS) and ensiled sorghum (ES) feedstocks. The sensitivity bars represent the pessimistic and optimistic results considering the sugar yield of 50% and 90% of the theoretical yield, respectively. The horizontal dashed lines represent (a) last 10-year (2009–2018) average gasoline selling price at the refinery gate of \$0.59 per L; and (b) the Renewable Fuel Standard (RFS) GHG emissions reduction target of 37.2 gCO<sub>2</sub>e per MJ (60% reduction relative to the petroleum baseline).<sup>33</sup>



water pretreatment of the same ES feedstock (Fig. 8). This large reduction in selling price is due to the improved sugar yield with the ensiled biomass and IL pretreatment (Table 1).

Cost, availability, and the quality of biomass feedstock are always important for the success of future cellulosic biorefineries, given that the biomass feedstock supply accounts for 40% of the total ethanol production cost. Biomass deconstruction, including pretreatment and hydrolysis, is another essential unit operation and is responsible for 23% of the total ethanol production cost. This cost contribution could reduce to 15% by utilizing the ensiled biomass sorghum feedstock at a low IL loading rate of 2.5 wt%. However, supplying the chopped/ensiled biomass sorghum for a large scale biorefinery located away from the field (>65 km) could be a challenge. This issue can be resolved by building the sugar production depots close to the field and transporting the concentrated sugar from the sugar depots to the biorefineries located away from the field. This allows utilization of the ensiled biomass feedstock regardless of the locations of biorefineries which not only helps for the economic and efficient biomass deconstruction but also lowers the overall feedstock supply cost.

Similar to the ethanol production cost, utilizing the ensiled biomass sorghum feedstock at the biorefinery minimizes the overall GHG footprint of ethanol by 8.2% and 7.8% at the IL loading rates of 5 wt% and 2.5 wt%, respectively, relative to the dry biomass sorghum feedstock at the same IL loading rates. These reductions are mainly due to improved biomass deconstruction efficiency with ensiled biomass (Fig. 3 and Table 1) and minimized neutralizing chemicals, such as sulfuric acid (Fig. 4). Regardless of biomass feedstock, the carbon footprint of bioethanol is reduced by 24% when IL loading rate is reduced by 2 times. This reduction, unlike ethanol production cost with dry biomass, is mainly due to reduced makeup IL required (which has a substantial GHG footprint) and a large carbon credit from net exports of electricity generated from residual solids and biogas available onsite (these credits will likely diminish as the U.S. grid mix shifts toward renewables). While the liquid hot water pretreatment is not economical relative to the IL pretreatment at the IL loading rate of 2.5 wt%, it reduces the overall GHG emissions by 65%. This large reduction in GHG emissions is due to the absence of IL and a large carbon credit from the onsite electricity generation, which results in net exports to the grid. A low biomass deconstruction efficiency of the hot water pretreatment results in a large fraction of the unutilized cellulose, hemicellulose, and lignin, which are ultimately combusted for onsite electricity generation. However, the GHG emissions credit from net electricity exports beyond the facility requirements (48% of the total electricity credits) is uncertain and dependent on how the U.S. national grid mix evolves in the next few decades.

We find that an IL-based biomass deconstruction process at a 5 wt% IL loading rate accounts for 51% of the net GHG emissions and this is reduced to 36% at an IL loading rate of 2.5 wt%. In addition to IL, the enzymes and sulfuric acid (used for pH adjustment) are non-negligible other sources of indirect GHG emissions for the biomass deconstruction process.

Future process improvements including hydrolysis at a low enzyme loading rate and elimination of the required pH adjustment step will further reduce the carbon footprint of the biorefinery.

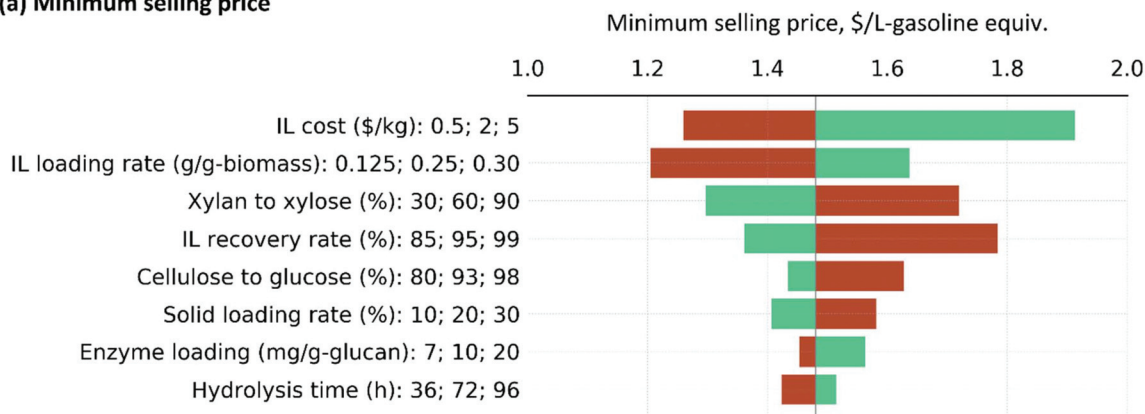
Unsurprisingly, the unoptimized bisabolene production in *R. toruloides* (Table 2) demonstrated in this study using the whole biomass hydrolysate in a one-pot configuration results in a very large minimum selling price of bisabolane in the range of \$25.7–31.5 per L-Jet A. Bisabolane is the hydrogenated product of bisabolene and can be used as a drop-in replacement for diesel and jet fuel.<sup>30,49</sup> The minimum selling price of bisabolane at the biorefinery gate obtained in this study is an order magnitude higher than the last 10-year (2009–2018) average selling price of Jet-A at the refinery gate of \$0.6 per L.<sup>30</sup> However, there are significant process improvement opportunities, including improving biomass deconstruction efficiency as well as titer, rate and yield of bisabolene that result in bisabolane at the market competitive price. Achieving sugar yield of 90% of the theoretical yield at a low ionic liquid and enzyme loadings as well as bisabolene yield of 90% of the theoretical yield could reduce the selling price of bisabolane to \$0.8 per L, which is quite close to the market price of Jet A.<sup>30</sup> This price could also possibly be pushed lower if government incentives for green fuels are created or if the lignin fraction of biomass is converted into a high value product instead of the process heat and electricity reported in this study. Some of these identified process improvement opportunities, such as a low IL and enzyme loading rates, are achieved in this study. In addition to biofuel, lipid content in *R. toruloides* (up to 60 wt%) can be recovered and transformed into value-added bioproducts/biofuels, generating additional revenue.<sup>52</sup> This potential opportunity will be explored in future studies to fully quantify the bisabolane production cost and associated GHG emissions using *R. toruloides*.

## 2.5. Cost and carbon footprint drivers associated with biomass deconstruction

Fig. 9 depicts the main cost and carbon footprint drivers associated with the biomass deconstruction process. IL cost is obviously influential to the minimum selling price of ethanol. This warrants a continuous research on identifying a cheap ILs for lignocellulosic biomass deconstruction. Additionally, changes in IL loading and recovery rates alter the amount of makeup IL required and therefore, both influence the selling price and GHG emissions of ethanol. Utilization of the ensiled biomass feedstock could be a stepping stone for a sustainable operation of cellulosic biorefineries in the future as it requires a low IL loading rate for effective biomass deconstruction. Future research efforts are required to achieve the targeted IL recovery rate of 99% with a minimal expenditure of cost and energy. Other influential parameters include glucose and xylose yields, solid and enzyme loading rates, and hydrolysis time. While the sugar yield directly alters the amount of biofuels, other parameters alter either the required amount of material (such as enzymes) or utilities and the size of process



## (a) Minimum selling price



## (b) Greenhouse gas emissions

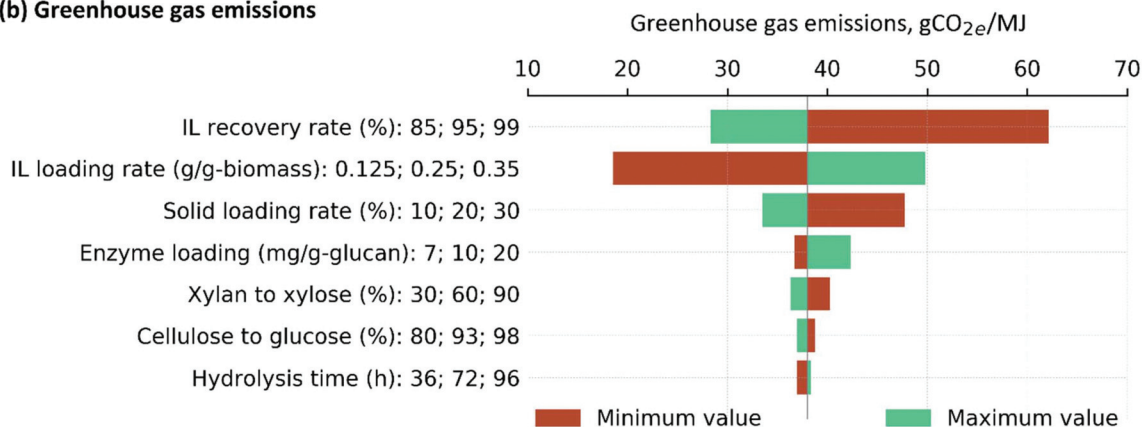


Fig. 9 Most influential input parameters associated with biomass deconstruction. This is a representative case considering the ensiled biomass sorghum at the IL loading rate of 5% (w/w).

equipment thereby influential to both cost and GHG emissions of ethanol.

The synergistic impacts of the most influential input parameters, including IL loading rate of 2.5% (w/w), IL recovery of 99%, sugar yield of 90% of the theoretical yield, solid loading rate of 30 wt%, enzyme loading rate of 7 mg of protein per g of glucan and hydrolysis time of 36 h reduces the overall ethanol selling price and GHG emissions to \$1.1 per L-gasoline-equivalent and 21.4 gCO<sub>2e</sub> per MJ, respectively. Future research that focuses on achieving these targets along with other system wide improvements are required to achieve a market-competitive price of ethanol (Fig. 8).

### 3. Conclusions

Ensiled biomass sorghum was found to be an effective feedstock for IL-based biorefineries. It enables a considerable reduction in the amount of IL used under mild pretreatment conditions, which results in a higher sugar yield relative to the unensiled biomass sorghum, thereby reducing the biofuel production cost and associated carbon footprint. The biomass deconstruction and bioconversion processes considered in

this study eliminate the requirement for IL separation prior to enzymatic hydrolysis and bioconversion processes. Additionally, the selected technology enables a consolidated one-pot process due to the use of an enzyme and microbe compatible ionic liquid, which has great potential to reduce the overall cost and the environmental footprint of the biorefinery. We find we can achieve a 16.7% reduction in ethanol production cost and 28.9% reduction in carbon footprint with the reported one-pot process that utilizes ensiled biomass relative to the conventional system that uses unensiled biomass. This process can be used to produce many other biofuels and bioproducts as long as the conversion host is able to tolerate and convert silage-derived organic acids and is a step towards establishing sustainable cellulosic biorefineries in the future.

### 4. Experimental

#### 4.1. Chemicals and feedstock

Ensiled sorghum biomass was obtained from a commercial silage pit on a dairy farm in the southern part of the San Joaquin Valley, California. Dried sorghum was supplied by Idaho National Laboratory (Idaho Falls, Idaho, USA). Ensiled



sorghum biomass samples were dried under sunlight prior to the experiments. Both dry ensiled and dry biomass were milled and passed through a 2 mm screen (Thomas-Wiley Model 4, Swedesboro, NJ). Commercial enzyme cocktails Cellic® CTec 3 and HTec 3 were generously provided by Novozymes (Davis, CA). Choline hydroxide (46% (w/w) in H<sub>2</sub>O) was purchased from Sigma-Aldrich (St. Louis, MO), L-lysine monohydrate was purchased from VWR and hydrochloric acid (36–37.5% (w/w)) was purchased from J.T. Baker (Phillipsburg, NJ) and used without further purification.

#### 4.2. Compositional analysis

The moisture content of both ensiled and dry sorghum biomass was measured gravimetrically after freeze-drying in a lyophilizer. Organic acids in the ensiled biomass were quantified by adding deionized water to biomass at a ratio of 10 : 1 (w/v) (*i.e.*, 10 mL of water into 1 g of biomass sample) and sonicated for 2–3 h. The collected extracts were filtered using 0.45 μm PTFE filters and analyzed using HPLC to characterize and quantify organic acids, including lactic acid and acetic acid. The pH of the extracts was determined using a pH meter (Mettler-Toledo International Inc., Columbus, OH). Extractives such as non-structural sugars, organic acids, proteins, inorganic material, chlorophyll, waxes, *etc.*, in both dry sorghum and dry ensiled sorghum biomass were removed using a three-step extraction process, including deionized water, followed by ethanol, and acetone.<sup>26</sup> The percentile extractive content of the dry biomass was determined by the dry weight differences before and after the extraction process. This value was also used to determine the overall raw biomass composition as other components of biomass, including glucan, xylan, and lignin, were determined based on the extractives-free biomass.

Structural composition of the extracted unpretreated biomass and pretreated biomass was determined according to NREL acidolysis protocols (LAP).<sup>27</sup> Briefly, 300 mg of biomass and 3 mL of 72% (w/w) H<sub>2</sub>SO<sub>4</sub> were incubated at 30 °C while shaking at 300 rpm for 1 h. The solution was diluted to 4% H<sub>2</sub>SO<sub>4</sub> with 84 mL of deionized water and autoclaved for 1 h at 121 °C. The reaction was quenched by placing samples into an ice bath and samples from the liquid fraction were collected for quantification of sugar monomers before removing the biomass by filtration. Acid soluble lignin was estimated by measuring the UV absorption of the acid hydrolysis supernatant at 240 nm using a UV-Vis spectrophotometer (Nanodrop 2000, Thermo Scientific, USA). Acid insoluble lignin was quantified gravimetrically from the solid after heating overnight at 105 °C (to obtain the weight of acid-insoluble lignin + ash) and then at 575 °C for at least 6 h (corresponding to the weight of ash).

#### 4.3. Ionic liquid synthesis

Lysine monohydrate (0.4 mol, 65.68 g) was weighed into a 500 mL round bottom flask and dissolved in 100 mL deionized water at room temperature to obtain a clear solution (light lime-yellow). Then the flask was mounted on an ice-bath (3–5 °C) and N<sub>2</sub> was purged for 20–30 min. Next 46% (w/w) of

choline hydroxide in water (0.4 mol, 105.15 g) was added dropwise to the lysine solution while maintaining the temperature of the ice-bath (3–5 °C). The mixture was stirred for 48 h at room temperature. Excess water was removed under reduced pressure and the mixture was added to acetonitrile/methanol (9 : 1, v/v) to remove the excess starting materials. Finally, the solvents were removed under reduced pressure and the mixture was freeze-dried to get the final product (yield ~95%, light orange).

#### 4.4. One-pot ionic liquid pretreatment

The one-pot biomass deconstruction process includes subsequent batch operations—pretreatment, pH adjustment, and enzymatic hydrolysis—in the same reactor without any separation (Fig. 10). The reactions comprised in the one-pot ionic liquid pretreatment were performed according to previously published methods<sup>21,28,29</sup> with the following modifications: the ensiled sorghum biomass (20% (w/w) initial pretreatment slurry) was mixed with [Ch][Lys] loadings of 10%, 5%, and 2.5% ((w/w) initial pretreatment slurry) in 60 mL capped pressure vials. All the pretreatment experiments were carried out in an oil bath at 140 °C for 3 h. Only one set of experiments were carried out at 95 °C to study the effect of the temperature on the IL pretreatments of [Ch][Lys] loadings of 5 and 2.5% (w/w). The same experimental conditions were used for dry sorghum biomass as a control.

Lignin removal during the IL pretreatment was analyzed for both dry and ensiled biomass sorghum. After the pretreatment, 30 mL of ethanol was added to the pretreated slurry and then transferred to a 50 mL conical tube and centrifuged at 4500 rpm to separate solids from liquid. The recovered solids were further washed with a mixture of ethanol and water (1 : 1) to remove any residual ILs or soluble materials. Finally, the recovered solid fraction was dried using the lyophilization before conducting compositional analysis. The difference between the lignin content before and after pretreatment was used to determine the extent of lignin during pretreatment.

Scaled-up pretreatment experiments for both ensiled and dry sorghum were carried out using a 1 L 4520 Parr benchtop reactor (Parr Instrument Company, Moline, IL, USA) equipped with three arms and a self-centering anchor with PTFE wiper blades.

#### 4.5. Enzymatic hydrolysis

After pretreatment, the pH of the resulting slurry was adjusted to pH 5 with 10 M hydrochloric acid. Commercial enzyme cocktails containing cellulase (Cellic® CTec3) and hemicellulase (Cellic® HTec3) mixed at a 9 : 1 (v/v) ratio were then directly added at an enzyme loading of 10 mg enzyme product per one gram of starting biomass. Three glass beads were added to each vial to facilitate mixing during enzymatic hydrolysis. Enzymatic hydrolysis was conducted at 50 °C for 72 h with constant agitation on an Enviro Genie SI-1200 rotator platform (Scientific Industries, Inc., Bohemia, NY).



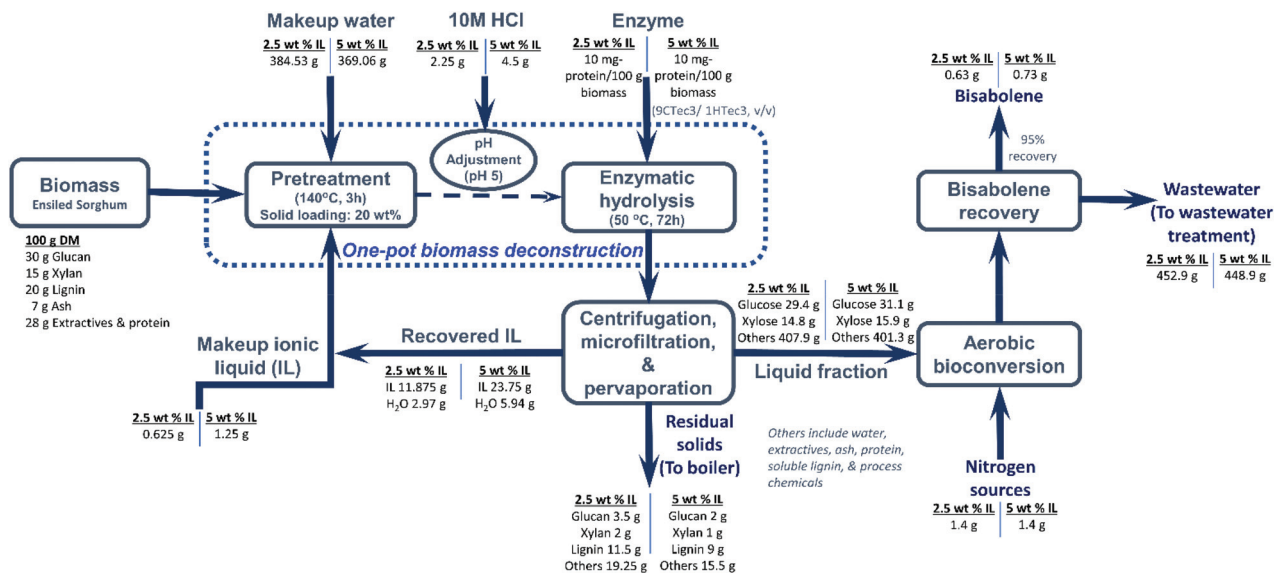


**Fig. 10** Process configuration and mass balance analysis considering bisabolene as a representative biofuel and ionic liquid and bisabolene recovery rates of 95%. Bisabolene production in *R. toruloides* using the whole biomass hydrolysate currently results in a low yield of bisabolene. The process demonstrated in this study requires further process optimization to improve titer, rate, and yield of bisabolene. In the current biorefinery model, the residual solid (mainly lignin) is routed to the boiler to generate process heat and electricity. However, if the lignin fraction of biomass could be upgraded into value-added products, the selling price and carbon footprint of bisabolene could be further reduced.<sup>30</sup>

#### 4.6. Analytical methods

Monomeric sugars and organic acids were quantified with an Agilent Technologies 1200 series HPLC system equipped with an Aminex HPX-87H column (BioRad Laboratories, USA), kept at 60 °C during analysis. 4 mM sulfuric acid was used as a mobile phase with a flow rate of 0.6 mL min<sup>-1</sup>. Prior to analysis, samples were filtered through 0.45 μm nylon centrifuge filters and 5 μL sample injection volumes were used. The compounds of interest were monitored using a refractive index detector and their concentrations were calculated by comparison of peak areas to standard curves made with pure compounds. To measure the amount of bisabolene produced in the cultivations (see section 4.7), the dodecane overlays at the end of the experiments were collected and diluted in pure dodecane spiked with 40 mg L<sup>-1</sup> of pentadecane, to be used as an internal standard. The samples were then analyzed by GC-MS using an Agilent Technologies 6890N system, equipped with a 5973-mass selective detector and a DB-5 ms column (30 m × 250 μm × 0.25 μm, Agilent Technologies, USA). Splitless 1 μL injections were used on a GC oven program consisting of 100 °C for 0.75 min, followed by a ramp of 20 °C per min until 300 °C, and held 1 min at 300 °C. Injector and MS quadrupole detector temperatures were 250 °C and 150 °C, respectively. The bisabolene concentrations reported here represent the concentrations that would be present in the aqueous phase of the cultivations (by dividing the concentrations measured in the dodecane layer by 4). Bisabolene was calculated by integration of the peak area values obtained in selective ion monitoring mode and compared to the areas obtained from a calibration curve made with pure bisabolene.

#### 4.7. Microbial cultivations

The yeast strain used in this work is deposited in the Joint BioEnergy Institute public registry and can be found in <https://public-registry.jbei.org> with the following ID: *Rhodospiridium toruloides* GB2.0, JBX\_086452. To perform fermentations, seed cultures were generated by inoculating the organism in 5 mL of YPD broth and incubating overnight at 30 °C and 200 rpm. Overnight cultures were diluted 10 times with fresh YPD media and grown until the mid-exponential phase prior to transferring to the cultivation media. Before inoculation, ammonium sulfate was added to clarified hydrolysates obtained from the one-pot process at a final concentration of 2 g L<sup>-1</sup>. A 1 : 9 v/v ratio of NH<sub>4</sub>SO<sub>4</sub> : hydrolysate was used to prepare hydrolysates at 90% final concentration and a 1 : 5 : 4 ratio v/v of NH<sub>4</sub>SO<sub>4</sub> : hydrolysate : water was used to prepare hydrolysates at 50% final concentration. For bisabolene production experiments, the initial pH of the media was adjusted to 7.5 using concentrated NaOH or H<sub>2</sub>SO<sub>4</sub>, filtered through 0.45 μm nylon centrifuge filters (VWR, USA), and transferred to 48-well Flower Plates (m2p labs, Germany) employing 780 μL of media, 20 μL of cells and 200 μL of a dodecane overlay, and covered with sterile AeraSeal films (Excel Scientific, USA). The plates were incubated for 7 days in a humidity-controlled incubator with orbital shaking at 900 rpm. The entire contents of each well were collected in Eppendorf tubes, where the dodecane layer, supernatant, and cells were separated by centrifugation and each fraction was kept frozen until analysis. The cell pellets were then resuspended in 800 μL of water, diluted forty-fold with water, and 100 μL were transferred to 96-well plates to measure final



optical density at 600 nm using a SpectraMax Plus 384 reader (Molecular Devices, USA). All cultivations were performed in triplicate. The percentile substrate utilization was calculated as the difference in concentration of glucose, xylose, or acetic acid at the beginning and end of the fermentation. The maximum grams of bisabolene that can be produced and the yields relative to the dry feedstock amounts were calculated using the following equations:

$$\text{Maximum bisabolene yield(g)} = [(\text{Glucose yield(g)} \times 0.252) + (\text{Xylose yield(g)} \times 0.210)]$$

$$\text{Yield relative to the theoretical maximum(\%)} = [(\text{Bisabolene yield(g)}/\text{Maximum bisabolene yield(g)}) \times 100]$$

$$\text{Total yield of bisabolene relative to dry feedstock(\%)} = [(\text{Bisabolene yield(g L}^{-1})/\text{Biomass loading(g L}^{-1})) \times (1/(\text{Hydrolysate dilution})) \times 100]$$

#### 4.8. Technoeconomic analysis and lifecycle assessment

Shifting from dry sorghum to an ensiled sorghum feedstock has associated cost and greenhouse gas (GHG) emissions tradeoffs. We evaluated these tradeoffs in the context of a hypothetical biomass sorghum-to-ethanol facility. Ethanol was modeled as the fuel product to facilitate comparisons with prior literature. For the dry and ensiled sorghum scenarios, we modeled a biorefinery sized to process the equivalent of 2000 dry metric tons of biomass per day (ensiled sorghum is transported and processed wet, so actual incoming mass will be greater). We calculated the minimum ethanol selling price and life-cycle GHG emissions per unit of ethanol produced to identify key cost and GHG drivers and provide results that can be compared with other published biomass-to-ethanol processes. We further determined the minimum selling price of bisabolene based on the proof-of-concept bisabolene production in *R. toruloides* demonstrated in this study. Bisabolene can be hydrogenated to produce bisabolane, which is a potential jet fuel blendstock.<sup>30</sup> The process models developed in SuperPro Designer are consistent with prior technoeconomic models of lignocellulosic biomass to ethanol<sup>31,32</sup> and bisabolene.<sup>30</sup> These models serve as the basis for the capital costs, operating costs, and the mass and energy balances that are used for the life-cycle GHG inventory. The biomass feedstock supply and handling as well as deconstruction stages are modified in this study. These are briefly discussed in the following paragraphs. The capital and operating parameters for other stages of the entire biofuel production chain are consistent with prior studies.<sup>30,32</sup>

The dry biomass supply system includes biomass sorghum production, windrowing, sun drying in the field, baling, stacking, transportation from the field to the biorefinery (including loading and unloading at each end), and storage next to the biorefinery under a tarp. The moisture content of biomass at the time of harvest is assumed to be 60%, which requires about 7 days of solar drying in the field to reach the expected

moisture content of biomass sorghum bales of 20%. Rainfall can complicate the dry-down process and increase costs and biomass storage losses. In contrast, the ensiled biomass sorghum feedstock supply system does not require drying in the field. Biomass is harvested in the form of chopped biomass by using a forage harvester, directly loaded on the truck, transported to the biorefinery (includes unloading), and ensiled next to the biorefinery in a bunker silo. The detailed input parameters considered for these two different biomass supply routes are documented in the ESI Tables S1 to S5.† The methods used to determine biomass feedstock supply cost and associated GHG emissions are consistent with a recent biomass sorghum feedstock supply model developed at JBEI/LBNL.<sup>33</sup>

Biomass feedstock handling at the biorefinery includes conveying, size reduction (only for dry biomass), and short-term storage. The size reduction step is not considered for the ensiled biomass as the particle size of the chopped biomass is assumed to be in the range of 0.12 to 1.9 cm, which can be directly fed into the pretreatment reactor. The biomass deconstruction stage, including pretreatment and enzymatic hydrolysis, is modified based on the methods and operating conditions considered for the experimental analysis as discussed earlier. Biocompatible and bio-derived ILs, such as cholinium lysinate, enable both biomass deconstruction and bioconversion processes to be conducted in a single vessel (one-pot) without any separation or water washing steps. The water-wash step of the conventional pretreatment processes can cause loss of the dissolved carbohydrates, such as hemicellulose, which are diverted to the wash stream, resulting in lower sugar yields relative to the starting biomass. However, in the one-pot configuration, all of the material is maintained in the system, enabling higher deconstruction and conversion efficiency.

For modeling purposes, we are deploying two different strategies for recovering lignin: (1) before bioconversion; and (2) after bioconversion. The former is used for aerobic bioconversion processes, such as bisabolene, and the latter is considered for anaerobic bioconversion, such as ethanol. For both cases, we recover the lignin fraction of biomass using centrifugation and a subsequent micro filtration. Either of these lignin recovery strategies can be deployed; however, energy consumption in the bioreactor will be significant in the presence of lignin and specifically for the aerobic bioconversion processes. Our experimental results show the lignin in solution does not appear to interfere with saccharification or bioconversion as evidenced by the high sugar yields and almost all sugar utilization during the bioconversion. Our prior works with [Ch][Lys] also show similar results.<sup>28,29,40</sup> Additionally, *R. toruloides* can consume low molecular weight lignin-derived compounds that are solubilized in the hydrolysates.<sup>23</sup> The recovered lignin is utilized for onsite energy generation. The IL is recovered *via* a pervaporation-based process.<sup>25,31,32</sup> We consider 95% IL recovery for the baseline analysis and 99% for the optimal future case.

Fig. 10 summarizes experimental data and process configuration considering bisabolene as a representative case. The



process equipment data are gathered from similar prior studies.<sup>31,34</sup> Following a rigorous material and energy balance for each unit operation, capital and operating costs as well as material and energy requirements for each stage of the entire biofuel production chain are determined. The economic evaluation parameters and the methods used to determine carbon footprint are documented in the ESI-S2.†

## Conflicts of interest

There are no conflicts to declare.

## Acknowledgements

This work was part of the DOE Joint BioEnergy Institute (<http://www.jbei.org>) supported by the U.S. Department of Energy, Office of Science, Office of Biological and Environmental Research, through contract DE-AC02-05CH11231 between Lawrence Berkeley National Laboratory and the U.S. Department of Energy. The United States Government retains and the publisher, by accepting the article for publication, acknowledges that the United States Government retains a non-exclusive, paid-up, irrevocable, worldwide license to publish or reproduce the published form of this manuscript, or allow others to do so, for United States Government purposes. The Department of Energy will provide public access to these results of federally sponsored research in accordance with the DOE Public Access Plan (<http://energy.gov/downloads/doe-public-access-plan>).

## References

- J. Holm and U. Lassi, in *Ionic liquids: applications and perspectives*, ed. A. Kokorin, InTech, 2011.
- G. W. Huber and A. Corma, *Angew. Chem., Int. Ed.*, 2007, **46**, 7184–7201.
- C. E. Wyman, B. E. Dale, R. T. Elander, M. Holtzapple, M. R. Ladisch and Y. Y. Lee, *Bioresour. Technol.*, 2005, **96**, 1959–1966.
- A. A. Elgharbawy, M. Z. Alam, M. Moniruzzaman and M. Goto, *Biochem. Eng. J.*, 2016, **109**, 252–267.
- D. M. Alonso, J. Q. Bond and J. A. Dumesic, *Green Chem.*, 2010, **12**, 1493.
- L. R. Lynd, C. E. Wyman and T. U. Gerngross, *Biotechnol. Prog.*, 1999, **15**, 777–793.
- C. E. Wyman, in *Handbook on bioethanol: production and utilization*, Routledge, 2018, pp. 1–18.
- D. Kim, *Molecules*, 2018, **23**, 309.
- J. C. Linden, L. L. Henk, V. G. Murphy, D. H. Smith, B. C. Gabrielsen, R. P. Tengerdy and L. Czako, *Biotechnol. Bioeng.*, 1987, **30**, 860–867.
- T. F. Bernardes, J. L. P. Daniel, A. T. Adesogan, T. A. McAllister, P. Drouin, L. G. Nussio, P. Huhtanen, G. F. Tremblay, G. Bélanger and Y. Cai, *J. Dairy Sci.*, 2018, **101**, 4001–4019.
- U. National Agricultural Statistics Service, *United States Department of Agriculture, Crop Production Annual Summary*, 2020.
- Z. Podkówka and L. Podkówka, *J. Cent. Eur. Agric.*, 2011, **12**, 294–303.
- T. R. Stefaniak, J. A. Dahlberg, B. W. Bean, N. Dighe, E. J. Wolfrum and W. L. Rooney, *Crop Sci.*, 2012, **52**, 1949.
- Y. Chen, R. R. Sharma-Shivappa and C. Chen, *Appl. Biochem. Biotechnol.*, 2007, **143**, 80–92.
- P. Oleskowicz-Popiel, A. B. Thomsen and J. E. Schmidt, *Biomass Bioenergy*, 2011, **35**, 2087–2092.
- M. Ambye-Jensen, S. T. Thomsen, Z. Kádár and A. S. Meyer, *Biotechnol. Biofuels*, 2013, **6**, 116.
- M. Ambye-Jensen, R. Balzarotti, S. T. Thomsen, C. Fonseca and Z. Kádár, *Biotechnol. Biofuels*, 2018, **11**, 336.
- M. Kawahata, K. Masaki, T. Fujii and H. Iefuji, *FEMS Yeast Res.*, 2006, **6**, 924–936.
- A. Ullah, R. Orij, S. Brul and G. J. Smits, *Appl. Environ. Microbiol.*, 2012, **78**, 8377–8387.
- V. Ward and L. Rehmann, in *Handbook of biorefinery research and technology*, ed. J. M. Park, Springer Netherlands, Dordrecht, 2018, 1–21.
- E. Sundstrom, J. Yaegashi, J. Yan, F. Masson, G. Papa, A. Rodriguez, M. Mirsiaghi, L. Liang, Q. He, D. Tanjore, T. R. Pray, S. Singh, B. Simmons, N. Sun, J. Magnuson and J. Gladden, *Green Chem.*, 2018, **20**, 2870–2879.
- J. Sun, N. V. S. N. Murthy Konda, R. Parthasarathi, T. Dutta, M. Valiev, F. Xu, B. A. Simmons and S. Singh, *Green Chem.*, 2017, **19**, 3152–3163.
- A. Rodriguez, N. Ersig, G. M. Geiselman, K. Seibel, B. A. Simmons, J. K. Magnuson, A. Eudes and J. M. Gladden, *Bioresour. Technol.*, 2019, **286**, 121365.
- T. Dutta, G. Papa, E. Wang, J. Sun, N. G. Isern, J. R. Cort, B. A. Simmons and S. Singh, *ACS Sustainable Chem. Eng.*, 2018, **6**, 3079–3090.
- J. Sun, J. Shi, N. V. S. N. Murthy Konda, D. Campos, D. Liu, S. Nemser, J. Shamshina, T. Dutta, P. Berton, G. Gurau, R. D. Rogers, B. A. Simmons and S. Singh, *Biotechnol. Biofuels*, 2017, **10**, 154.
- S. D. Mansfield, H. Kim, F. Lu and J. Ralph, *Nat. Protoc.*, 2012, **7**, 1579–1589.
- A. Sluiter, B. Hames, R. Ruiz, C. Scarlata, J. Sluiter, D. Templeton and D. Crocker, *Laboratory Analytical Procedure (LAP)*, 2012.
- F. Xu, J. Sun, N. V. S. N. M. Konda, J. Shi, T. Dutta, C. D. Scown, B. A. Simmons and S. Singh, *Energy Environ. Sci.*, 2016, **9**, 1042–1049.
- J. Shi, J. M. Gladden, N. Sathitsuksanoh, P. Kambam, L. Sandoval, D. Mitra, S. Zhang, A. George, S. W. Singer, B. A. Simmons and S. Singh, *Green Chem.*, 2013, **15**, 2579.
- N. R. Baral, O. Kavvada, D. Mendez-Perez, A. Mukhopadhyay, T. S. Lee, B. A. Simmons and C. D. Scown, *Energy Environ. Sci.*, 2019, **12**, 807–824.



- 31 B. Neupane, N. V. S. N. M. Konda, S. Singh, B. A. Simmons and C. D. Scown, *ACS Sustainable Chem. Eng.*, 2017, **5**, 10176–10185.
- 32 D. Humbird, R. Davis, L. Tao, C. Kinchin, D. Hsu, A. Aden, P. Schoen, J. Lukas, B. Olthof, M. Worley, D. Sexton and D. Dudgeon, *Process Design and Economics for Biochemical Conversion of Lignocellulosic Biomass to Ethanol: Dilute-Acid Pretreatment and Enzymatic Hydrolysis of Corn Stover*, National Renewable Energy Laboratory (NREL), Golden, CO (United States), 2011.
- 33 N. R. Baral, O. Kavvada, D. Mendez-Perez, A. Mukhopadhyay, T. S. Lee, B. Simmons and C. D. Scown, *ACS Sustainable Chem. Eng.*, 2019, **7**, 5434–15444.
- 34 N. R. Baral, C. Quiroz-Arita and T. H. Bradley, *Environ. Sci. Technol.*, 2018, **52**, 14528–14537.
- 35 W. A. Dewar, P. McDonald and R. Whittenbury, *J. Sci. Food Agric.*, 1963, **14**, 411–417.
- 36 J. S. de Oliveira, E. M. Santos and A. P. M. dos Santos, in *Advances in silage production and utilization*, ed. T. Da Silva and E. M. Santos, InTech, 2016.
- 37 V. L. Nsereko, B. K. Smiley, W. M. Rutherford, A. Spielbauer, K. J. Forrester, G. H. Hettinger, E. K. Harman and B. R. Harman, *Anim. Feed Sci. Technol.*, 2008, **145**, 122–135.
- 38 P. McDonald, A. R. Henderson and S. J. E. Heron, in *The Biochemistry of Silage*, Scholium Intl, 1991.
- 39 X. D. Hou, J. Xu, N. Li and M.-H. Zong, *Biotechnol. Bioeng.*, 2015, **112**, 65–73.
- 40 N. Sun, R. Parthasarathi, A. M. Socha, J. Shi, S. Zhang, V. Stavila, K. L. Sale, B. A. Simmons and S. Singh, *Green Chem.*, 2014, **16**, 2546–2557.
- 41 Q. P. Liu, X. D. Hou, N. Li and M. H. Zong, *Green Chem.*, 2012, **14**, 304–307.
- 42 J. Xu, M. H. Thomsen and A. B. Thomsen, *J. Biotechnol.*, 2009, **139**, 300–305.
- 43 A. M. Johnson, H. Kim, J. Ralph and S. D. Mansfield, *Biotechnol. Biofuels*, 2017, **10**, 48.
- 44 G. Papa, J. Kirby, N. V. S. N. Murthy Konda, K. Tran, S. Singh, J. D. Keasling, G. F. Peter and B. A. Simmons, *Green Chem.*, 2017, **19**, 1117–1127.
- 45 L. J. Jönsson and C. Martín, *Bioresour. Technol.*, 2016, **199**, 103–112.
- 46 Q. Fei, M. O'Brien, R. Nelson, X. Chen, A. Lowell and N. Dowe, *Biotechnol. Biofuels*, 2016, **9**, 130.
- 47 J. Yaegashi, J. Kirby, M. Ito, J. Sun, T. Dutta, M. Mirsiaghi, E. R. Sundstrom, A. Rodriguez, E. Baidoo, D. Tanjore, T. Pray, K. Sale, S. Singh, J. D. Keasling, B. A. Simmons, S. W. Singer, J. K. Magnuson, A. P. Arkin, J. M. Skerker and J. M. Gladden, *Biotechnol. Biofuels*, 2017, **10**, 241.
- 48 M. Wehrs, J. M. Gladden, Y. Liu, L. Platz, J.-P. Prah, J. Moon, G. Papa, E. Sundstrom, G. M. Geiselman, D. Tanjore, J. D. Keasling, T. R. Pray, B. A. Simmons and A. Mukhopadhyay, *Green Chem.*, 2019, **21**, 3394–3406.
- 49 P. P. Peralta-Yahya, M. Ouellet, R. Chan, A. Mukhopadhyay, J. D. Keasling and T. S. Lee, *Nat. Commun.*, 2011, **2**, 483.
- 50 B. Özyaydin, H. Burd, T. S. Lee and J. D. Keasling, *Metab. Eng.*, 2013, **15**, 174–183.
- 51 E. M. Kim, H. M. Woo, T. Tian, S. Yilmaz, P. Javidpour, J. D. Keasling and T. S. Lee, *Metab. Eng.*, 2017, **44**, 325–336.
- 52 M. Masri, D. Garbe, N. Mehlmer and T. Brück, *Energy Environ. Sci.*, 2019, **12**, 2717–2732.

